

Research Paper

Calculation for Acoustic Radiation Force from Rectangular Weakly Focusing Transducer Using the Ray Acoustic Model

Lili YU⁽¹⁾, Shuchang QIAO⁽¹⁾, Wende SHOU^{(2),(3)*}, Junhua LI⁽⁴⁾⁽¹⁾ Merchant Marine College, Shanghai Maritime University
Shanghai 201306, China⁽²⁾ School of Biomedical Engineering, Shanghai Jiao Tong University
Shanghai 200030, China⁽³⁾ Shanghai Institute of Ultrasound in Medicine
Shanghai 200233, China

*Corresponding Author e-mail: wdshou@163.com

⁽⁴⁾ College of Ocean Science and Engineering, Shanghai Maritime University
Shanghai 201306, China

(received April 13, 2021; accepted December 10, 2021)

Based on the ray acoustic model, a new relationship between the radiation force and the acoustic power is studied for a rectangular weakly focusing transducer. The effect of pressure reflection coefficient on this model is discussed. For a totally absorbing target, an approximate closed-form expression is also derived and the performance of this model is compared with that of the far-field integration model. The numerical results show that the agreement is excellent with these two models, which can be both used for correction of measured results, but the formula based on the ray acoustic model can be applied more widely in practice because of its simpler expression. The experimental results show further the effectiveness of the relationship between radiation force and acoustic power for rectangular weakly focusing transducer based on the ray acoustic model. The results presented in this paper are important for application of ultrasound transducers in therapy.

Keywords: radiation force calculation; ray acoustic model; rectangular weakly focusing transducer; far-field integration.



Copyright © 2022 L. Yu et al.
This is an open-access article distributed under the terms of the Creative Commons Attribution-ShareAlike 4.0 International (CC BY-SA 4.0) <https://creativecommons.org/licenses/by-sa/4.0/> which permits use, distribution, and reproduction in any medium, provided that the article is properly cited, the use is non-commercial, and no modifications or adaptations are made.

1. Introduction

The measurement of acoustic power generated by a therapeutic ultrasound transducer is essential to the safety and effectiveness of the treatment (SHAW, HODNETT, 2008; SHAW *et al.*, 2015; 2016; HEKKENBERG *et al.*, 2001). The measurement method recommended by the International Electrotechnical Commission (IEC) as the first choice is a radiation force balance, in which the radiation force acting on a target inserted in the field is measured by means of a balance (GÉLAT, SHAW, 2015; IEC61161, 2013; MURUVADA *et al.*, 2007). For a perfectly absorbing target, the relationship between the measured radiation force (F) and the total time-averaged acoustic power (P)

for unfocused field with the plane-progressive wave is (IEC61161, 2013, p. 30)

$$\frac{cF}{P} = 1, \quad (1)$$

where c is the speed of sound in the propagation medium (normally degassed water). For focused field with a spherically concave focusing transducer, an approximate closed-form result for a large absorber is (IEC61161, 2013, p. 31)

$$\frac{cF}{P} = \frac{1 + \cos \alpha}{2}, \quad (2)$$

where α is half-aperture angle. The Eq. (2) was derived originally by Beissner from the far-field integra-

tion method (BEISSNER, 1987). After then, based on the ray acoustic model, SHOU *et al.* (1998; 2006) obtained the same result on a totally absorbing target in the focused acoustic field. Over the last 30 years, the radiation force balance (RFB) means has successfully been verified in some international comparisons (BEISSNER *et al.*, 1996; CIVALE *et al.*, 2018), and the related details have repeatedly been described in literatures (BEISSNER, 2010; QIAN *et al.*, 2010; XU *et al.*, 2019).

With the widespread use of diagnostic ultrasonic equipment equipped with rectangular linear-array transducers, it appears highly desirable to derive the relationships between force and power for rectangular cases. For a rectangular weakly focusing transducer, an approximate closed-form result of radiation force calculation acting on a totally absorbing target based on the far-field integration model was published in related literatures (BEISSNER, 2008; IEC61161, 2013, p. 32) and is expressed as follows:

$$\frac{cF}{P} = \frac{\sin \alpha \cdot \arctan(\cos \alpha \cdot \tan \beta)}{2\arcsin(\sin \alpha \cdot \sin \beta)} + \frac{\sin \beta \cdot \arctan(\cos \beta \cdot \tan \alpha)}{2\arcsin(\sin \alpha \cdot \sin \beta)}, \quad (3)$$

where α is half-aperture angle for the x - z plane, and β is half-aperture angle for the y - z plane. So far, however, there are few reported results referring to how to verify this closed-form solution (Eq. (3)) by other models.

In this paper, for a rectangular weakly focusing transducer and a reflecting target with convex cone-shaped, the relationship between the total radiation force and the time-averaged acoustic power in a continuous wave was obtained based on the ray acoustic model. Then, an approximate closed-form expression of radiation force calculation acting on a totally absorbing target was also derived from the same model. To verify the reliability of ray acoustic model, the comparison between the ray acoustic model and the far-field integration model was conducted subsequently. The experiments were also performed for a rectangular weakly focusing transducer to validate the effectiveness of ray acoustic model.

2. Theory calculation

2.1. Ray acoustic model

Based on the assumption of ray acoustics, i.e. the acoustic intensity on the transducer's surface is a constant, I_0 ; the diameter of focus is zero; the sound energy has no loss in propagation and the sound energy flow is identical in the same solid angle passing the focus, the focused acoustic field of a rectangular focusing transducer is shown in Fig. 1.

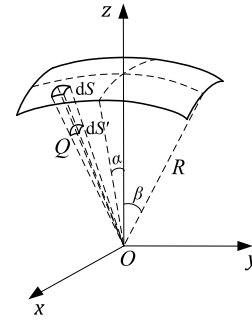


Fig. 1. Focused acoustic field of rectangular focusing transducer.

The radius of curvature of transducer or the geometrical focal length is R . The half-aperture angle is α in the x - z plane, and is β in the y - z plane. A surface element area, dS' is perpendicular to the acoustic ray at point Q where the acoustic intensity is I . The solid angle constructed by focus O and dS' extends from the focus to the surface of the sound source and forms a projected surface element area, dS on the radiation face of the transducer, where the acoustic intensity is I_0 . When diffraction is neglected, i.e. in the geometric or high-frequency limit, the following equation can be obtained:

$$I dS' = I_0 dS. \quad (4)$$

The geometries of element area dS are shown at (R, θ_A, θ_B) in Fig. 2, where $dl_1 = R_A d\theta_A$ and $dl_2 = R_B d\theta_B$ are the arc-length of element area dS in the $y = O_2$ plane, and in the $x = O_1$ plane, respectively. $R_A = R \cos \theta_B$ and $R_B = R \cos \theta_A$ are the radius of curvature of dl_1 and dl_2 , respectively. $d\theta_A$ and $d\theta_B$ are the open angle of dl_1 and dl_2 , respectively. Thus, dS can be expressed as

$$\begin{aligned} dS &= dl_1 \cdot dl_2 = R_A d\theta_A \cdot R_B d\theta_B \\ &= R^2 \cos \theta_A \cos \theta_B d\theta_A d\theta_B. \end{aligned} \quad (5)$$

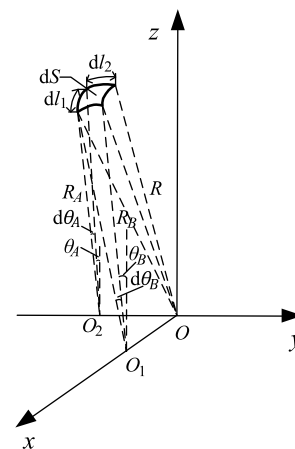


Fig. 2. The geometries of element area dS for the spherical coordinate system.

According to Langiven's radiation pressure principle, the impulse flow energy density of a plane wave, i.e. radiation pressure P_r , can be expressed as: $P_r = I/c$, where, I is the acoustic intensity of a plane wave, in W/m^2 , c is the speed of sound in medium (water), in m/s .

A convex conical reflecting target is located at a position between the transducer and the focus in the above acoustic field and it should be large enough to intersect all sound energy. The symmetrical axis of the target is aligned to symmetrical axis of the transducer's surface. Figure 3 shows the geometrics of the rectangular focusing transducer and the target.

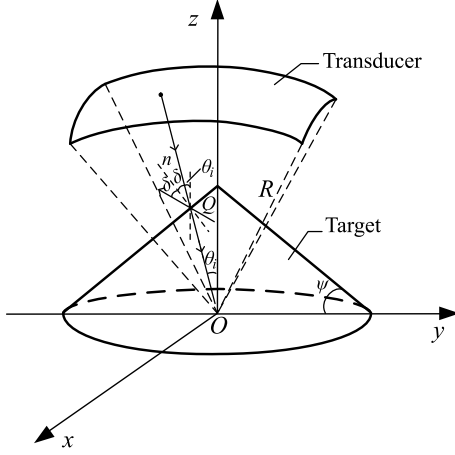


Fig. 3. The geometrics of the rectangular focusing transducer and the target.

Assuming an acoustic ray with the acoustic intensity I injects to a point Q on the target, the acoustic ray can be regarded as a very thin sound beam of plane wave. The normal direction perpendicular to the surface of target is denoted as n , and the incidence angle between the acoustic ray and normal direction of target's surface is δ . The angle between the acoustic ray and z -axis is equal to θ_i . Thus, the dip angle of the target's surface is $\Psi = \delta + \theta_i$. At point Q , the axial component of the incidence sound impulse flow energy density is, $I \cos \theta_i / c$ and the axial component of the reflecting sound impulse flow energy density is $r_f^2 I \cos(2\delta + \theta_i) / c$, where r_f is the pressure reflection coefficient on the interface between water and the target, and $0 \leq r_f \leq 1$.

According to the impulse conservation law, the axial component of impulse flow energy density or radiation pressure acting at point Q on the target for a plane wave can be expressed as

$$\begin{aligned} P_r &= \frac{I}{c} [\cos \theta_i + r_f^2 \cdot \cos(2\delta + \theta_i)] \\ &= \frac{I}{c} [\cos \theta_i + r_f^2 \cdot \cos(2\psi - \theta_i)]. \end{aligned} \quad (6)$$

The whole focused sound beam is made up of numerous thin sound beams. The cross-section of a thin

sound beam at the incidence point Q is dS' and each thin sound beam can be seen as a thin plane wave beam. The beam acting on the reflecting target can be treated as an axial component of the radiation force dF on dS' caused by the thin sound beam. It can be expressed as

$$dF = \frac{I}{c} [\cos \theta_i + r_f^2 \cdot \cos(2\psi - \theta_i)] \cdot dS'. \quad (7)$$

It is assumed that the surface element area dS' is perpendicular to the incidence acoustic ray at point Q , and the another surface element area dS on the radiation surface of the transducer is in the same focused solid angle. According to Eq. (4), the axial component of the radiation force at point Q can be expressed as

$$dF = \frac{I_0}{c} [\cos \theta_i + r_f^2 \cdot \cos(2\psi - \theta_i)] \cdot dS. \quad (8)$$

The component of radiation force perpendicular to the axial direction acting on the target sums up to be equal to zero because the surface of the transducer and target are symmetrical with respect to the z -axis. Thus, the total radiation force acting on the whole target equals to the surface integral of dF on dS or dS' , i.e. $F = \int_{S'} dF = \int_S dF$. Besides, the following result can be obtained with $R \cos \theta_i = R_A \cos \theta_A = R_B \cos \theta_B$ in Figs 2 and 3 for the spherical coordinate system:

$$\cos \theta_i = \cos \theta_A \cos \theta_B. \quad (9)$$

Therefore, the sum component of radiation force action on the target, i.e. the total radiation force, can be calculated from the following equation:

$$\begin{aligned} F &= \frac{I_0 R^2}{c} \left(\int_{-\alpha}^{\alpha} \int_{-\beta}^{\beta} \cos^2 \theta_A \cdot \cos^2 \theta_B \cdot d\theta_A d\theta_B \right. \\ &\quad + \cos 2\psi \int_{-\alpha}^{\alpha} \int_{-\beta}^{\beta} r_f^2 \cdot \cos^2 \theta_A \cdot \cos^2 \theta_B \cdot d\theta_A d\theta_B \\ &\quad + \sin 2\psi \int_{-\alpha}^{\alpha} \int_{-\beta}^{\beta} r_f^2 \cdot \sqrt{1 - \cos^2 \theta_A \cdot \cos^2 \theta_B} \\ &\quad \left. \cdot \cos \theta_A \cdot \cos \theta_B \cdot d\theta_A d\theta_B \right). \end{aligned} \quad (10)$$

Accounting for the acoustic power of the sound source

$$\begin{aligned} P &= \int I_0 \cdot dS \\ &= I_0 \int_{-\alpha}^{\alpha} \int_{-\beta}^{\beta} \cos \theta_A \cdot \cos \theta_B \cdot d\theta_A d\theta_B \\ &= 4I_0 \cdot R^2 \cdot \sin \alpha \cdot \sin \beta. \end{aligned} \quad (11)$$

The following formula can be obtained from both Eq. (10) and Eq. (11):

$$\begin{aligned} \frac{cF}{P} = & \frac{1}{4 \sin \alpha \cdot \sin \beta} \left(\int_{-\alpha}^{\alpha} \int_{-\beta}^{\beta} \cos^2 \theta_A \cdot \cos^2 \theta_B \cdot d\theta_A d\theta_B \right. \\ & + \cos 2\psi \int_{-\alpha}^{\alpha} \int_{-\beta}^{\beta} r_f^2 \cdot \cos^2 \theta_A \cdot \cos^2 \theta_B \cdot d\theta_A d\theta_B \\ & + \sin 2\psi \int_{-\alpha}^{\alpha} \int_{-\beta}^{\beta} r_f^2 \cdot \sqrt{1 - \cos^2 \theta_A \cdot \cos^2 \theta_B} \\ & \left. \cdot \cos \theta_A \cdot \cos \theta_B \cdot d\theta_A d\theta_B \right). \end{aligned} \quad (12)$$

Thus, for a totally reflecting target ($r_f = 1$) with convex cone-shaped, the relationship between the total radiation force and the time-averaged acoustic power in a continuous wave field can be expressed as

$$\begin{aligned} \frac{cF}{P} = & \frac{1}{16 \sin \alpha \cdot \sin \beta} \\ & \cdot \left[(1 + \cos 2\psi) (2\alpha + \sin 2\alpha) (2\beta + \sin 2\beta) \right. \\ & + 4 \sin 2\psi \int_{-\alpha}^{\alpha} \int_{-\beta}^{\beta} \sqrt{1 - \cos^2 \theta_A \cdot \cos^2 \theta_B} \\ & \left. \cdot \cos \theta_A \cdot \cos \theta_B \cdot d\theta_A d\theta_B \right]. \end{aligned} \quad (13)$$

The angles α and β in the Eq. (13) are to be used in radians. Figure 4 shows the relationships between the ratio cF/P and the dip angle Ψ of target's surface for Eq. (13) with three different angles γ , which is used to characterize the transducer size and is chosen to be a geometric mean $\gamma = \sqrt{\alpha \cdot \beta}$. With Ψ increasing, the ratio cF/P gradually decreases. It should be noted that

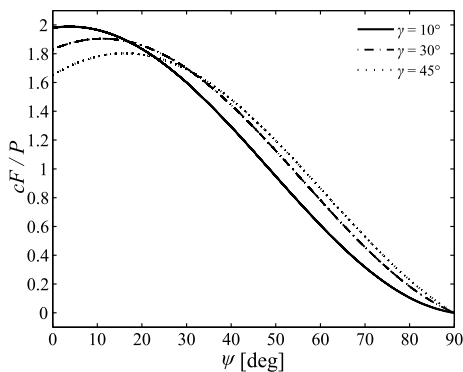


Fig. 4. Radiation force ration cF/P versus dip angle ψ for different angles γ on a totally reflecting target.

the reflected acoustic beams could return to surface of transducer for a totally reflecting target ($r_f = 1$). It will cause the change of impedance of transducer and the instability of output power, which leads to the failure of measurements.

2.2. Pressure reflection coefficient on a plane absorbing target

In practice measurements, a plane absorbing target ($\Psi = 0^\circ$) is usually applied for measurements, in which the pressure reflection coefficient r_f is very small value, but is not equal to zero.

When the sound wave is incident from the water onto a plane absorbing target, both the longitudinal wave and the transverse wave exist at the water-target interface. Thus, the reflection coefficient $r(\theta_i)$ is a function of the incident angle θ_i and can be expressed as (IEC TS 62903, 2018, p. 20)

$$r(\theta_i) = \left| \frac{z_{2L} \cos^2 2\theta_{iT} + z_{2T} \sin^2 2\theta_{iT} - z_{1L}}{z_{2L} \cos^2 2\theta_{iT} + z_{2T} \sin^2 2\theta_{iT} + z_{1L}} \right|, \quad (14)$$

where $r(\theta_i)$ is a function of incident angle θ_i with $\theta_i = \arccos(\cos \theta_A \cos \theta_B)$. $z_{1L} = \frac{\rho_1 c_{1L}}{\cos \theta_i}$, $z_{2L} = \frac{\rho_2 c_{2L}}{\cos \theta_{tL}}$, and $z_{2T} = \frac{\rho_2 c_{2T}}{\cos \theta_{tT}}$ are the normal acoustic impedances of the longitudinal wave for water, the longitudinal wave for the target, and the transverse wave for the target, respectively. $\theta_{tL} = \arcsin\left(\frac{c_{2L}}{c_{1L}} \sin \theta_i\right)$ and $\theta_{tT} = \arcsin\left(\frac{c_{2T}}{c_{1L}} \sin \theta_i\right)$ are the refraction angles of the longitudinal wave and the transverse wave, respectively; and ρ_1 and ρ_2 are the density of water and that of the target. c_{1L} , c_{2L} , and c_{2T} are the sound speeds of the longitudinal wave for water, the longitudinal wave for the target, and the transverse wave for the target, respectively.

Thus, there are two cases worthy of consideration. As the most simple case, the pressure reflection coefficient r_f can be regarded as an independent constant with the perpendicular incidence ($\theta_i = 0^\circ$), i.e. $r_f = r(\theta_i)|_{\theta_i=0^\circ}$, the following formula can be derived from Eq. (12) for a plane absorbing target ($\Psi = 0^\circ$):

$$\begin{aligned} \frac{cF}{P} = & \frac{1}{16 \sin \alpha \cdot \sin \beta} \\ & \cdot \left[(1 + r^2(\theta_i)|_{\theta_i=0^\circ}) (2\alpha + \sin 2\alpha) (2\beta + \sin 2\beta) \right], \end{aligned} \quad (15)$$

where the angle α and β are to be used in radians.

However, if the pressure reflection coefficient r_f is not an independent constant and is as a function of incident angle θ_i , i.e. $r_f = r(\theta_i)$, the follow relationship can be obtained from Eq. (12) for a plane absorbing target ($\Psi = 0^\circ$):

$$\frac{cF}{P} = \frac{1}{16 \sin \alpha \cdot \sin \beta} \left[(2\alpha + \sin 2\alpha)(2\beta + \sin 2\beta) + 4 \int_{-\alpha}^{\alpha} \int_{-\beta}^{\beta} r^2(\theta_i) \cdot \cos^2 \theta_A \cdot \cos^2 \theta_B \cdot d\theta_A d\theta_B \right], \quad (16)$$

where the angle α and β are to be used in radians.

In this study, a plane absorbing target is made of rubber with $\rho_2 = 1200 \text{ kg/m}^3$, $c_{2L} = 2300 \text{ m/s}$ and $c_{2T} = 940 \text{ m/s}$. The parameters are $\rho_1 = 1000 \text{ g/m}^3$ and $c_1 = 1492 \text{ m/s}$ for water. Thus, $r(\theta_i)|_{\theta_i=0^\circ} \approx 0.298$ can be obtained from Eq. (14). Figure 5 shows that the calculation results for Eqs (15) and (16), respectively. For $\gamma < 30^\circ$, the maximum error is not greater than 0.4% between Eq. (15) and Eq. (16), whose agreement is very well.

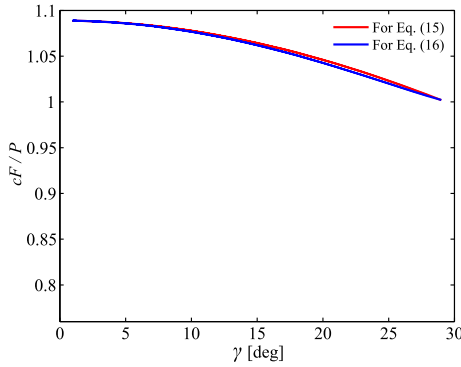


Fig. 5. Radiation force ratio cF/P versus angle γ for pressure reflection coefficients r_f on a plane absorbing target.

To simplify the calculations in practical application, Eq. (15) can be employed if the parameters of a plane absorbing target are obtained, or the following formula can be further obtained from Eq. (12) for a totally absorbing target ($r_f = 0$):

$$\frac{cF}{P} = \frac{(2\alpha + \sin 2\alpha)(2\beta + \sin 2\beta)}{16 \sin \alpha \cdot \sin \beta}, \quad (17)$$

where the angle α and β are to be used in radians.

2.3. Comparison of two models

For the same totally absorbing target, the expression of Eq. (17) for the ray acoustic model is obviously different from that of Eq. (3) for far-field integration model. Consequently, the comparison between Eq. (17) and Eq. (3) is conducted for $\gamma \leq 45^\circ$ and as a function of the nominal F -number (i.e. $1/(2 \sin \gamma)$). The computation results are presented in Figs 6 and 7, where the relative deviation between Eq. (17) and Eq. (3) is not greater than 0.7% for $\gamma \leq 45^\circ$ (i.e. F -number ≥ 0.707) and is not greater than 0.3% for $\gamma \leq 30^\circ$ (i.e. F -number ≥ 1.0).

Then, the results of further comparison are listed in Table 1 for $5^\circ \leq \alpha \leq 45^\circ$ with $\beta = 10^\circ, 30^\circ$, and 45° .

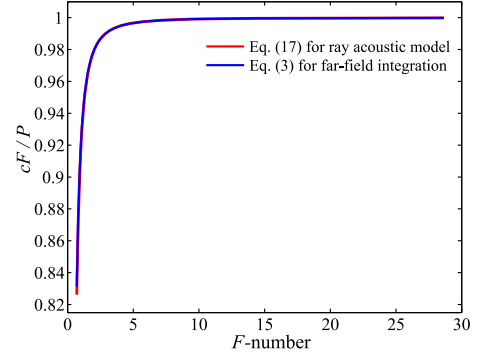


Fig. 6. Radiation force ratio cF/P versus the nominal F -number for a totally absorbing target.

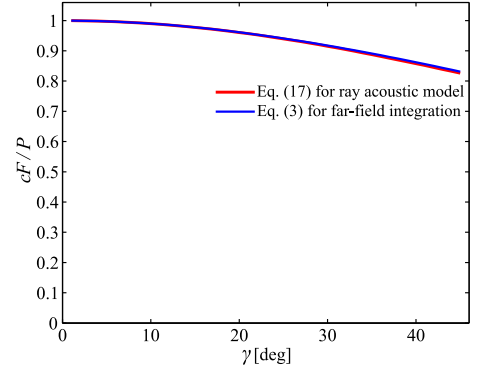


Fig. 7. Radiation force ratio cF/P versus angle γ for a totally absorbing target.

From Table 1, the relative deviation is not greater than 0.11% for $\beta = 10^\circ$, 0.46% for $\beta = 30^\circ$, and 0.61% for $\beta = 45^\circ$.

Table 1. Comparison of the relationships between radiation force and acoustic power on a totally absorbing target for a rectangular weakly focusing transducer.

α ($^\circ$)	$\beta = 10^\circ$		$\beta = 30^\circ$		$\beta = 45^\circ$	
	cF/P^*	cF/P^{**}	cF/P^*	cF/P^{**}	cF/P^*	cF/P^{**}
5	0.994	0.994	0.955	0.955	0.908	0.908
10	0.990	0.990	0.952	0.952	0.904	0.905
15	0.984	0.984	0.946	0.947	0.899	0.900
20	0.975	0.975	0.938	0.939	0.891	0.893
25	0.964	0.965	0.927	0.929	0.881	0.884
30	0.952	0.952	0.915	0.917	0.869	0.873
35	0.938	0.938	0.901	0.904	0.856	0.861
40	0.921	0.922	0.886	0.889	0.842	0.847
45	0.904	0.905	0.869	0.873	0.826	0.831

* $\frac{cF}{P} = \frac{(2\alpha + \sin 2\alpha)(2\beta + \sin 2\beta)}{16 \sin \alpha \cdot \sin \beta}$ for a ray acoustic model.

** $\frac{cF}{P} = \frac{\sin \alpha \cdot \arctan(\cos \alpha \cdot \tan \beta) + \sin \beta \cdot \arctan(\cos \beta \cdot \tan \alpha)}{2 \arcsin(\sin \alpha \cdot \sin \beta)}$ for a far-field integration model.

Therefore, the agreement is excellent with these two methods, which can be both employed for radiation force calculation of a rectangular weakly focusing

transducer. Certainly, due to the simpler expression, Eq. (17) based on the ray acoustic model should be more widely applied in practice.

In the above, we have discussed the case that there is focusing in both planes. However, if there is focusing only in one plane, e.g. only in the x - z plane, this can formally be expressed by $\beta = 0^\circ$, but then either Eq. (17) or Eq. (3) becomes indeterminate. The problem can be solved using L'Hospital's rule. For the ray acoustic model, Eq. (17) should be derived as follows:

$$\begin{aligned} \frac{cF}{P} &= \lim_{\beta \rightarrow 0} \frac{(2\alpha + \sin 2\alpha)(2\beta + \sin 2\beta)}{16 \sin \alpha \cdot \sin \beta} \\ &= \frac{\alpha + \sin \alpha \cdot \cos \alpha}{2 \sin \alpha}. \end{aligned} \quad (18)$$

Also for the far-field integration model, Eq. (3) should be derived as follows (IEC61161, 2013, p. 32)

$$\begin{aligned} \frac{cF}{P} &= \lim_{\beta \rightarrow 0} \frac{\sin \alpha \cdot \arctan(\cos \alpha \cdot \tan \beta) + \sin \beta \cdot \arctan(\cos \beta \cdot \tan \alpha)}{2 \arcsin(\sin \alpha \cdot \sin \beta)} \\ &= \frac{\alpha + \sin \alpha \cdot \cos \alpha}{2 \sin \alpha}. \end{aligned} \quad (19)$$

The angle α in the Eqs (18) and (19) is to be used in radians. Obviously, the closed-form expression of Eq. (18) based on the ray acoustic model is exactly the same as Eq. (19) based on the far-field integration model. This result can be applied for radiation force calculation acting on a totally absorbing target for a cylindrical concave transducer (YU *et al.*, 2012).

3. Experimental measurements

To validate the effectiveness of ray acoustic model, the setup of the experiment is shown in Fig. 8.

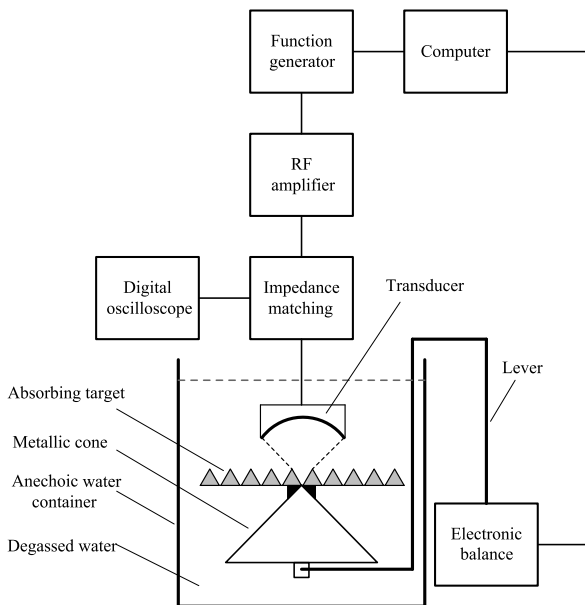


Fig. 8. Experimental setup for the radiation force balance (RFB) method.

An air-backed rectangular focusing transducer with a 3.9-MHz resonance frequency, a 10-mm focal length, and $\alpha = \beta = 30^\circ$ is used for measurement. The absorbing target in the water container was supported at the tip of a metallic cone. The transducer was positioned so that it radiated downward onto the target. The radiant power is directly proportional to the total downward force on the target. This force was transferred through the lever to the electronic balance (Model UPM-DT-1, Ohmic Instruments Co., Easton, MD). The driving electronics consisted of a function generator (Model 33220A, Agilent Tech., Palo Alto, CA) and power amplifier (Model RSG-I, Changzhou Rishige Electronics Technology Co., Ltd., Changzhou, China). The operation of the radiation force in the balance system was accomplished through a computer. The driving voltage of the transducer was measured with a digital oscilloscope (Model DSO-X 2012A, KEYSIGHT Tech., Santa Rosa, CA). Moreover, the plane-absorbing target was made of Ultrasonic Absorber UA-1 (the Institute of Acoustics, Chinese Academy of Sciences) with a 30-mm diameter and 5-mm thickness of silicone rubber. The distance between the absorbing target and the transducer should not be greater than the focal length of the transducer. In the comparison of experimental results, the radiation conductance G_r is defined as (IEC TS 62903, 2018, p. 34)

$$G_r = \frac{P}{U_{T_{\text{rms}}}^2}, \quad (20)$$

where $U_{T_{\text{rms}}}$ is the root mean square of the driving voltage of the transducer and G_r is in Siemens (S). Often, G_r is used in the laboratory to compare the acoustic power measured by different methods from the same transducer. In the experiment, G_r was determined by the least square method in the measured acoustic power vs. the square driving voltage.

The measurements were conducted in degassed water at 24°C. Figure 9 shows the measured acous-

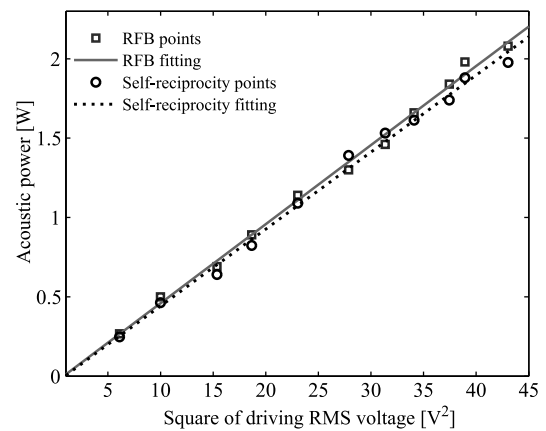


Fig. 9. Acoustic power comparison between RFB and self-reciprocity methods for rectangular weakly focusing transducer ($f = 3.9$ MHz, $R = 10$ mm, and $\alpha = \beta = 30^\circ$).

tic power with a rectangular weakly focusing transducer at 3.9 MHz using two different methods, i.e. the RFB method and the self-reciprocity method (IEC TS 62903, 2018, p. 36), for comparison. The measured results of RFB method were corrected by Eq. (17) based on the ray acoustic model. The radiation conductance measured by RFB and self-reciprocity were 49.8 mS and 48.5 mS, respectively. The average deviation of the RFB from the self-reciprocity method in radiation conductance measurements was 2.68%, and the maximum deviation of measured acoustic power by both methods was 8.09%.

From Fig. 9, the results obtained by RFB and self-reciprocity methods are generally consistent. Therefore, the closed-form expressions of cF/P are valid for acoustic power measurements of rectangular weakly focusing transducer based on a ray acoustic model.

4. Conclusion

In conclusion, the new relationships between radiation force and acoustic power for a rectangular weakly focusing transducer are studied. The formula (12) based on the ray acoustic model is obtained and can be applied in correction of the measured acoustic power of a rectangular weakly focusing transducer on a reflecting or absorbing target. For a totally absorbing target, an approximate closed-form expression of cF/P (Eq. (17)) based on the ray acoustic model is also derived and compared with the other formula (3), which is based on the far-field integration model. The numerical results show that the agreement is excellent between these two models, which can be both used for correction of measured results with a rectangular weakly focusing transducer. Moreover, the Eq. (17) can be applied more widely in practice because of its simpler expression. Finally, the experimental results showed further the effectiveness of the relationship between radiation force and acoustic power for a rectangular weakly focusing transducer based on the ray acoustic model. The results presented in this paper are important for application of ultrasound transducers in therapy.

Acknowledgments

This paper was supported by National Natural Science Foundation of China under Grant No. 39970209 and No. 51209133.

References

- BEISSNER K. (1987), Radiation force calculations, *Acta Acustica united with Acustica*, **62**(4): 255–263.
- BEISSNER K. (2008), Radiation force calculations for ultrasonic fields from rectangular weakly focusing transducers, *The Journal of the Acoustical Society of America*, **124**(4): 1941–1949, doi: 10.1121/1.2968687.
- BEISSNER K. (2010), Minimum radiation force target size for power measurements in focused ultrasonic fields with circular symmetry, *The Journal of the Acoustical Society of America*, **128**(6): 3355–3362, doi: 10.1121/1.3505105.
- BEISSNER K., OOSTERBAAN W.A., HEKKENBERG R.T., SHAW A. (1996), European intercomparison of ultrasonic power measurements, *Acta Acustica united with Acustica*, **82**(3): 450–458.
- CIVALE J., RIVENS J., SHAW A., TER HAAR G. (2018), Focused ultrasound transducer spatial peak intensity estimation: a comparison of methods, *Physics in Medicine and Biology*, **63**(5): 055015, doi: 10.1088/1361-6560/aaaf01.
- GÉLAT P., SHAW A. (2015), Relationship between acoustic power and acoustic radiation force on absorbing and reflecting targets for spherically focusing radiators, *Ultrasound in Medicine and Biology*, **41**(3): 832–844, doi: 10.1016/j.ultrasmedbio.2014.09.021.
- HEKKENBERG R.T., BEISSNER K., ZEQRIRI B., BEZEMER R.A., HODNETT M. (2001), Validated ultrasonic power measurements up to 20 W, *Ultrasound in Medicine and Biology*, **27**(3): 427–438, doi: 10.1016/S0301-5629(00)00344-6.
- IEC61161 (2013), *Ultrasonics – Power measurement-Radiation force balances and performance requirements*, 3rd ed., International Electrotechnical Commission.
- IEC TS 62903 (2018), *Ultrasonics – Measurements of electroacoustical parameters and acoustic output power of spherically curved transducers using the self-reciprocity method*, 1st ed., International Electrotechnical Commission.
- MURUVADA S., HARRIS G.R., HERMAN B.A. (2007), Acoustic power calibration of high-intensity focused ultrasound transducers using a radiation force technique, *The Journal of the Acoustical Society of America*, **121**(3): 1434–1439, doi: 10.1121/1.2431332.
- QIAN Z.W., ZHU Z.M., YE S.G., JIANG W.H., ZHU H.Q., YU J.S. (2010), Radiation force on absorbing targets and power measurements of a high intensity focused ultrasound (HIFU) source, *Science China Physics, Mechanics and Astronomy*, **53**(10): 1780–1787, doi: 10.1007/s11433-010-4117-8.
- SHAW A., HODNETT M. (2008), Calibration and measurement issues for therapeutic ultrasound, *Ultrasonics*, **48**(4): 234–252, doi: 10.1016/j.ultras.2007.10.010.
- SHAW A., MARTIN E., HALLER J., TER HAAR G. (2016), Equipment, measurement and dose – a survey for therapeutic ultrasound, *Journal of Therapeutic Ultrasound*, **4**(1): 7, doi: 10.1186/s40349-016-0051-1.

14. SHAW A., TER HAAR G., HALLER J., WILKENS V. (2015), Towards a dosimetric framework for therapeutic ultrasound, *International Journal of Hyperthermia*, **31**(2): 182–192, doi: 10.3109/02656736.2014.997311.
15. SHOU W.D. *et al.* (1998), Radiation force calculation of focused ultrasound and its experiment in high intensity focused ultrasound [in Chinese], *Technical Acoustics*, **17**(4): 145–147.
16. SHOU W.D. *et al.* (2006), Acoustic power measurement of high intensity focused ultrasound in medicine based on radiation force, *Ultrasonics*, **44**(Supplement): e17–e20, doi: 10.1016/j.ultras.2006.06.034.
17. XU J.X., GUI Y.F., MA J.M. (2019), Calculation and optimization of acoustic radiation force produced by a two-dimensional transducer array, *Journal of Applied Physics*, **125**(13): 134905, doi: 10.1063/1.5055362.
18. YU L.L., SHOU W.D., HUI C., HU B. (2012), Radiation force calculation and acoustic power measurement for a cylindrical concave transducer based on the ray acoustic model, *Journal of the Korean Physical Society*, **61**(4): 544–550, doi: 10.3938/jkps.61.544.